CHEMISTRY
A EUROPEAN JOURNAL

DOI: 10.1002/chem.200701519

Synthesis, Molecular Structure and Properties of the $[H_{6-n}Ni_{30}C_4(CO)_{34}(CdCl)_2]^{n-}$ ($n=3$–6) Bimetallic Carbide Carbonyl Cluster: A Model for the Growth of Noncompact Interstitial Metal Carbides

Alessandro Bernardi,[a] Cristina Femoni,[a] Maria Carmela Iapalucci,[a] Giuliano Longoni,[a] Fabrizio Ranuzzi,[a] Stefano Zacchini,*[a] Piero Zanello,[b] and Serena Fedi[b]

Abstract: Reaction of the $[Ni_9C(CO)_{17}]^{2-}$ dianion with $CdCl_2{\cdot}2.5\,H_2O$ in THF affords the novel bimetallic Ni–Cd carbide carbonyl clusters $[H_{6-n}Ni_{30}C_4(CO)_{34}(\mu_5\text{-}CdCl)_2]^{n-}$ ($n=3$–6), which undergo several protonation–deprotonation equilibria in solution depending on the basicity of the solvent or upon addition of acids or bases. Although the occurrence in solution of these equilibria complicates the pertinent electrochemical studies on their electron-transfer activity, they clearly indicate that the clusters $[H_{6-n}Ni_{30}C_4(CO)_{34}(\mu_5\text{-}CdCl)_2]^{n-}$ ($n=3$–6), as well as the structurally related $[H_{6-n}Ni_{34}C_4(CO)_{38}]^{n-}$ ($n=4$–6), undergo reversible or partially reversible redox processes and provide circumstantial and unambiguous evidence for the presence of hydrides for $n=3$, 4 and 5. Three of the $[H_{6-n}Ni_{30}C_4(CO)_{34}(\mu_5\text{-}CdCl)_2]^{n-}$ anions ($n=4$–6) have been structurally characterized in their $[NMe_3(CH_2Ph)]_4[H_2Ni_{30}C_4(CO)_{34}(CdCl)_2]{\cdot}2\,COMe_2$, $[NEt_4]_5[HNi_{30}C_4(CO)_{34}(CdCl)_2]{\cdot}2\,MeCN$ and $[NMe_4]_6[Ni_{30}C_4(CO)_{34}(CdCl)_2]{\cdot}6\,MeCN$ salts, respectively. All three anions display almost identical geometries and bonding parameters, probably because charge effects are minimized by delocalization over such a large metal carbonyl anion. Moreover, the $Ni_{30}C_4$ core in these Ni–Cd carbide clusters is identical within experimental error to those present in the $[HNi_{34}C_4(CO)_{38}]^{5-}$ and $[Ni_{35}C_4(CO)_{39}]^{6-}$ species, suggesting that the stepwise assembly of their nickel carbide cores may represent a general pathway of growth of nickel polycarbide clusters. The fact that the $[H_{6-n}Ni_{30}C_4(CO)_{34}(\mu_5\text{-}CdCl)_2]^{n-}$($n$=4–6) anions display two valence electrons more than the structurally related $[H_{6-n}Ni_{34}C_4(CO)_{38}]^{n-}$ ($n=4$–6) species has been rationalized by extended Hückel molecular orbital (EHMO) analysis.

Keywords: carbides · cluster compounds · EHMO calculations · electrochemistry · structure elucidation

Introduction

Inclusion of heteroatoms into the metal cages of molecular clusters as well as in extended metal lattices is widely documented and finds its most important application in the preparation of metal–heteroatom alloys.[1] A renewed interest in this area arises from the possibility of alloying metals and heteroatoms at the nanolevel, besides the potential applications to metal cluster chemistry and bulk metallurgy. There might be considerable impact on many areas of science and engineering such as the nanosciences, catalysis, and materials sciences.[2] For instance, Fe-, Co-, and Ni-catalyzed production of carbon nanotubes is thought to proceed via formation of metal carbide nanoparticles.[3]

The stabilizing effect of interstitial main group elements in metal carbonyl clusters was demonstrated several years ago, and is exemplified by the preparation and characteriza-

[a] A. Bernardi, Dr. C. Femoni, Prof. M. C. Iapalucci, Prof. G. Longoni, Dr. F. Ranuzzi, Dr. S. Zacchini
Dipartimento di Chimica Fisica ed Inorganica
Università di Bologna, Viale Risorgimento 4-40136 Bologna (Italy)
Fax: (+39) 051-209-3690
E-mail: zac@ms.fci.unibo.it

[b] Prof. P. Zanello, Dr. S. Fedi
Dipartimento di Chimica
Università di Siena, Via De Gasperi 2, Siena (Italy)

Supporting information comprising full lists of the individual bond lengths and main average values for $[NMe_3(CH_2Ph)]_4[H_2Ni_{30}C_4(CO)_{34}(CdCl)_2]{\cdot}2\,COMe_2$, $[NEt_4]_5[HNi_{30}C_4(CO)_{34}(CdCl)_2]{\cdot}2\,MeCN$, and $[NMe_4]_6[Ni_{30}C_4(CO)_{34}(CdCl)_2]{\cdot}6\,MeCN$ for this article is available on the WWW under http://www.chemeurj.org/ or from the author.

tion of numerous species containing a large variety of interstitial atoms, for example, B, C, N, Si, P, As, Bi, Sb, Sn, and Ge.[4–7] Among these, metal carbide carbonyl clusters have attracted great attention, because of their structural, electronic and chemical properties.[1,4,8] In particular, the ability of carbon atoms to stabilize metal clusters is well documented in the chemistry of nickel carbonyls.[9] Thus, nickel forms only a few low-nuclearity homometallic clusters, among which $[Ni_5(CO)_{12}]^{2-}$, $[Ni_6(CO)_{12}]^{2-}$, $[Ni_9(CO)_{18}]^{2-}$, and $[H_xNi_{12}(CO)_{21}]^{(4-x)-}$ ($x=0$–2) have been structurally characterized.[10,11] Conversely, several high-nuclearity nickel carbide carbonyl clusters are known, and nuclearities up to 38 have been reported. The structurally characterized compounds include monocarbide (for example, $[Ni_7C(CO)_{16}]^{2-}$,[12] $[Ni_8C(CO)_{16}]^{2-}$ and $[Ni_9C(CO)_{17}]^{2-}$[13]), tetracarbide (for example, $[HNi_{34}C_4(CO)_{38}]^{5-}$ and $[Ni_{35}C_4(CO)_{39}]^{6-}$[14]), and hexacarbide species (for example, $[Ni_{32}C_6(CO)_{36}]^{6-}$ and $[HNi_{38}C_6(CO)_{42}]^{5-}$[15,16]). All the above species contain isolated carbide atoms encapsulated either in a trigonal-prismatic or in a square-antiprismatic nickel cavity. In addition, there are several nickel carbido carbonyl clusters containing C_2 moieties, featuring short C–C contacts, encapsulated in more expanded, less regular nickel cavities (for example, $[Ni_{10}C_2(CO)_{15}]^{2-}$,[17] $[Ni_{11}C_2(CO)_{15}]^{4-}$, $[Ni_{12}C_2(CO)_{16}]^{4-}$,[12] and $[Ni_{16}(C_2)_2(CO)_{23}]^{4-}$[18]). All the above species have been synthesized mainly by reaction of $[Ni_6(CO)_{12}]^{2-}$ with perhalohydrocarbons such as CCl_4, C_2Cl_4, C_2Cl_6, and C_3Cl_8. The rich chemistry of nickel carbide carbonyl clusters contrasts with the low solubility of carbon in bulk nickel metal, the metastable Ni_3C being the only phase reported to date.[19]

Further interest in these molecular compounds comes from the behavior of the highest-nuclearity species, namely $[Ni_{32}C_6(CO)_{36}]^{6-}$ and $[HNi_{38}C_6(CO)_{42}]^{5-}$, as electron sinks as good as C_{60}[20] and their ability to be sequentially and reversibly reduced to species with a charge of −10, whereas the lowest-nuclearity nickel carbides do not withstand any redox change.[15,16] Moreover, their capacitance of around 0.7 aF per molecule[4] is comparable with that of quasi monodispersed gold colloids stabilized by thiols.[21–23] The appearance of new electronic properties on nanometric molecular clusters has suggested that metal clusters stabilized in a ligand shell are valid candidates for assembly in functional devices for data storage and could potentially represent the ultimate solution for miniaturization in microelectronics and nanolithography.[24–25]

It was therefore of interest to develop the chemistry of high-nuclearity nickel carbide clusters further, to obtain increasingly effective molecular nanocapacitors and to gain a better insight into the structure and growth of heterometallic nanoparticles. An alternative approach to high-nuclearity nickel carbide carbonyl clusters was suggested by the selective synthesis of high-nuclearity Rh carbonyl clusters by oxidation in mild conditions of $[Rh_7(CO)_{16}]^{3-}$ with $MX_n{\cdot}yH_2O$ hydrated Lewis acids, among them the $CdCl_2{\cdot}2.5H_2O$ salt:[26] so we investigated the mild oxidation of the preformed $[Ni_9C(CO)_{17}]^{2-}$ species with hydrated $CdCl_2$ salts. We report here the synthesis, structural, and spectroscopic characterization of the series of bimetallic nickel carbide carbonyl clusters of general formula $[H_{6-n}Ni_{30}C_4(CO)_{34}(\mu_5\text{-}CdCl)_2]^{n-}$ ($n=3$–6). Their electrochemical behavior has also been investigated and compared with that of the structurally related but nonisoelectronic $[H_{6-n}Ni_{34}C_4(CO)_{38}]^{n-}$ ($n=3$–6) derivatives. The difference in electron counts of the two series of compounds has been rationalized by EHMO analysis.

Results and Discussion

Synthesis and characterization of the $[H_{6-n}Ni_{30}C_4(CO)_{34}(CdCl)_2]^{n-}$ ($n=3$–6) clusters: The reaction of the $[Ni_9C(CO)_{17}]^{2-}$ dianion, as its $[NEt_4]^+$, $[NMe_4]^+$, or $[NMe_3(CH_2Ph)]^+$ salt, with $CdCl_2{\cdot}2.5H_2O$ in THF leads to formation of a brown precipitate over a period of 3 h. The material is soluble in acetone, acetonitrile, and DMF; the solution of the sample in acetone displays infrared carbonyl absorptions at 2019 (s) and 1874 (m) cm^{-1}, whereas those in acetonitrile and DMF display a similar pattern with bands shifted at 2008 (s) and 1862 (ms) cm^{-1}, and 1996 (s) and 1855 (m) cm^{-1}, respectively. The above differences in absorption frequencies were hardly compatible with simple solvent effects and suggested the possible occurrence of deprotonation equilibria in the miscellaneous solvents, as a function of their basicity. In keeping with this suggestion, crystallization of the brown precipitate in acetone/isopropanol and acetonitrile/diisopropyl ether mixtures afforded crystals of $[H_{6-n}Ni_{30}C_4(CO)_{34}(CdCl)_2]^{n-}$ salts with $n=4$ and 5, respectively. In particular, crystals of the $[NMe_3(CH_2Ph)]_4[H_2Ni_{30}C_4(CO)_{34}(CdCl)_2]{\cdot}2\,COMe_2$ and $[NEt_4]_5[HNi_{30}C_4(CO)_{34}(CdCl)_2]{\cdot}2\,MeCN$ salts were found to be suitable for X-ray analysis. Significantly, both products are soluble in acetonitrile and show most intense IR carbonyl absorptions at 2008 (s) and 1862 (m) cm^{-1}. However, the crystals of $[NMe_3(CH_2Ph)]_4[H_2Ni_{30}C_4(CO)_{34}(CdCl)_2]{\cdot}2\,COMe_2$ are also soluble in acetone, in which they display their most intense infrared carbonyl absorptions at 2019 (s) and 1874 (m) cm^{-1}, and weak shoulders at 2008 (s) and 1862 (m) cm^{-1}, owing to some deprotonation. These observations confirm, first, the occurrence in the miscellaneous solvents of protonation–deprotonation equilibria, which are shifted to one or another $[H_{6-n}Ni_{30}C_4(CO)_{34}(CdCl)_2]^{n-}$ species, as a function of the relative basicity of the solvent. Second, as shown in Scheme 1, the above observations lead us to conclude that the species present in the less basic solvent acetone is the dihydride tetra-anion $[H_2Ni_{30}C_4(CO)_{34}(CdCl)_2]^{4-}$, which is converted to a great extent into the monohydride penta-anion $[HNi_{30}C_4(CO)_{34}(CdCl)_2]^{5-}$ by dissolving its salts in the more basic acetonitrile. Further partial deprotonation of the latter occurs in DMF and leads to significant concentration of the $[Ni_{30}C_4(CO)_{34}(CdCl)_2]^{6-}$ hexa-anion. A pure solution of $[Ni_{30}C_4(CO)_{34}(CdCl)_2]^{6-}$ can be obtained only by shifting the equilibrium to the left by addition of solid $NaHCO_3$ as a mild deprotonating reagent. Crystals suitable for X-ray analysis of the $[NMe_4]_6$-

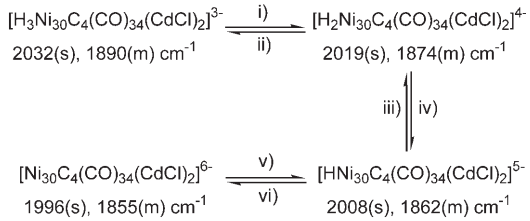

Scheme 1. i) Dissolution in acetone without acids; ii) $+H_2SO_4$ in acetone; iii) $+ H_2SO_4$ in acetone; iv) dissolution in CH_3CN; v) $+ H_2O$ in CH_3CN or DMF; vi) $+ NaHCO_3$ or 4,4'-bipyr4idine in CH_3CN or DMF.

$[Ni_{30}C_4(CO)_{34}(CdCl)_2]$·6 MeCN salt, which contains the $[Ni_{30}C_4(CO)_{34}(CdCl)_2]^{6-}$ hexa-anion, have been obtained by layering diisopropyl ether on a solution of a mixture of $[HNi_{30}C_4(CO)_{34}(CdCl)_2]^{5-}$ and $[Ni_{30}C_4(CO)_{34}(CdCl)_2]^{6-}$ in MeCN in the presence of a slight excess of a mild deprotonating reagent such as 4,4′-bipyridine.

Finally, reaction of $[Ni_{30}C_4(CO)_{34}(CdCl)_2]^{6-}$ in DMF with a strong base such as NaOH results in a complex mixture of decomposition products. Precipitation with H_2O or treatment with acids of the mixture regenerates only very minor amounts of the starting $[H_{6-n}Ni_{30}C_4(CO)_{34}(CdCl)_2]^{n-}$ ($n=3$–6) clusters and has enabled isolation of species such as $[HNi_{34}C_4(CO)_{38})]^{5-}$ and the new bimetallic $[HNi_{32}C_4(CO)_{36}(CdCl)]^{6-}$ (C. Femoni, M. C. Iapalucci, G. Longoni, S. Zacchini, unpublished work). These results confirm that no further simple deprotonation occurs beyond formation of the hexa-anion and suggests that the subsequent attack of a strong base such as NaOH is addressed toward the $CdCl^+$ fragments coordinated to the cluster.

The equilibrium at the bottom of Scheme 1 is partially reversed by water, whereas regeneration of the $[H_2Ni_{30}C_4(CO)_{34}(CdCl)_2]^{4-}$ species requires addition of a roughly stoichiometric amount of aqueous H_2SO_4. As shown in Scheme 1, IR monitoring indicates that protonation of the $[H_2Ni_{30}C_4(CO)_{34}(CdCl)_2]^{4-}$ tetra-anion in acetone proceeds further to give the corresponding $[H_3Ni_{30}C_4(CO)_{34}(CdCl)_2]^{3-}$ tri-anion, which is still sufficiently stable to be isolated in the solid state by evaporation of the reaction solution and washing of the residue with isopropanol.

Significantly, treatment of $[Ni_{30}C_4(CO)_{34}(CdCl)_2]^{6-}$ with stoichiometric amounts of oxidizing agents such as Ag^+, I_2, or tropylium tetrafluoroborate leads only to irreversible decomposition of the starting material. The absence of spectroscopic evidence for the possible existence of $[Ni_{30}C_4(CO)_{34}(CdCl)_2]^{n-}$ ($n<6$) further supports the conclusion that the charge changes reported in Scheme 1 arise from protonation–deprotonation reactions and not from redox processes.

The behavior of the $[H_{6-n}Ni_{30}C_4(CO)_{34}(\mu_5\text{-}CdCl)_2]^{n-}$ ($n=$ 3–6) species illustrated in Scheme 1 parallels those of the previously reported $[H_{6-n}Ni_{34}C_4(CO)_{38}]^{n-}$ clusters.[14] As in those earlier examples, all attempts to determine the number or even the presence of hydride atoms by ^1H NMR had no success. No signal, other than those due to the tetra-substituted ammonium cations and solvents, was detectable even by adopting long delays (as much as 60 s) between pulses in order to avoid signal saturation, by running the spectra in nondeuterated solvents to hinder H–D exchange, by performing variable-temperature experiments to slow down possible dynamic processes, or by trying to enhance the hydride signals by employing very concentrated solutions or acquiring several thousands of scans. The lack of any response by high-nuclearity clusters by means of ^1H NMR spectroscopy is, unfortunately, a rather general phenomenon. It is also the case for miscellaneous metal carbonyl clusters such as $[H_{6-n}Ni_{32}C_6(CO)_{36}]^{n-}$, $[H_{6-n}Ni_{38}C_6(CO)_{42}]^{n-}$,[15,16] $[H_{6-n}Ni_{36}Pt_4(CO)_{44}]^{n-}$,[27] $[H_{6-n}Ni_{38}Pt_6(CO)_{48}]^{n-}$,[28] and $[H_{8-n}Rh_{22}(CO)_{35}]^{n-}$ ($n=3$–5).[29] To our knowledge, the only high-nuclearity cluster whose hydrides have been clearly detected by ^1H NMR is $H_{12}Pd_{28}Pt_{13}(CO)_{27}(PMe_3)(PPh_3)_{12}$.[30] Related difficulties in observing all the expected NMR signals are also documented for colloidal metal nanoparticles stabilized by ligands.[31]

Attempts to gather direct evidence for the presence of hydrogen in $[H_{6-n}Ni_{34}C_4(CO)_{38}]^{n-}$ and $[H_{6-n}Ni_{30}C_4(CO)_{34}(\mu_5\text{-}CdCl)_2]^{n-}$ ($n=3$–5) by ESI-MS have been inconclusive. The ESI mass spectrum of $[NMe_4]_4[H_2Ni_{30}C_4(CO)_{34}(CdCl)_2]$ (Figure 1) displays several multiplets in the m/z regions of

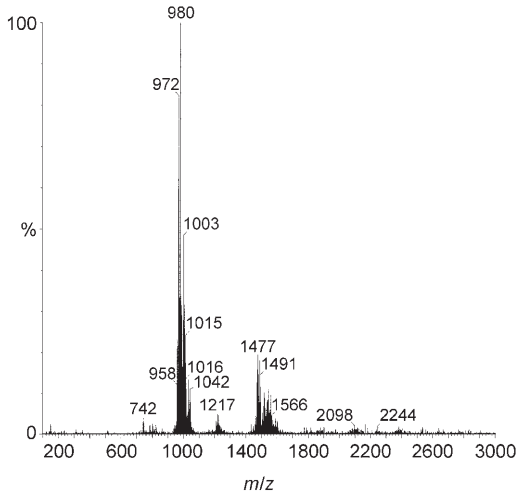

Figure 1. ESI mass spectrum of $[NMe_4]_4[H_2Ni_{30}C_4(CO)_{34}(CdCl)_2]$ in CH_3CN.

$z=2$ and 3. The strongest multiplets (relative intensities in parentheses) are centered at $m/z=980$ (100), 1003 (50), 1033 (20) and 1477 (20), 1490 (20), and 1545 (13) and can be attributed to $[Ni_{30}C_4(CO)_{30}(CdCl)_2]^{3-}$, $[Ni_{30}C_5(CO)_{32}(CdCl)_2]^{3-}$, $\{[NMe_4][Ni_{30}C_4(CO)_{33}(CdCl)_2]\}^{3-}$ and $[Ni_{30}C_5(CO)_{30}(CdCl)_2]^{2-}$, $[Ni_{30}C_4(CO)_{31}(CdCl)_2]^{2-}$, and $\{[NMe_4][Ni_{30}C_5(CO)_{32}(CdCl)_2]\}^{2-}$, respectively. The complexity of the natural isotopic composition of Ni, Cd, and Cl, the close values of the average mass of one Cd atom (112.41) and 4 CO (112.04), and CO elimination or disproportionation processes hamper unequivocal interpretation of the multiplets and gathering of unambiguous evidence for the presence of hydrides.

As a result, the number of hydride atoms assigned relies on chemical, rather than spectroscopic behavior: that is, the number of reversible deprotonation steps occurring in solution under mild conditions (vide supra). Further circumstantial proof of the presence of hydride atoms in these miscellaneous anions is provided by the electrochemical studies reported below.

The synthesis of $[H_2Ni_{30}C_4(CO)_{34}(CdCl)_2]^{4-}$ from $[Ni_9C(CO)_{17}]^{2-}$ and $CdCl_2{\cdot}2.5\,H_2O$ is explained formally by Equation (1), in which the H^+ ions are derived from the acidity of the coordinated water of $CdCl_2{\cdot}2.5\,H_2O$. Equation (1) is in keeping with the experimental observation that the only by-product detectable by IR is $Ni(CO)_4$.

$$4\,[Ni_9C(CO)_{17}]^{2-} + 2\,CdCl_2 + 2\,H^+ \rightarrow [H_2Ni_{30}C_4(CO)_{34}(CdCl)_2]^{4-} + 10\,CO + 2\,Cl^- + 6\,Ni(CO)_4 \quad (1)$$

As confirmed by comparing the structures of $[H_{6-n}Ni_{30}C_4(CO)_{34}(CdCl)_2]^{n-}$ ($n=4$–6) and $[HNi_{34}C_4(CO)_{38}]^{5-}$ (see next section), Equation (1) parallels Equation (2). Indeed, addition of protonic acids to $[Ni_9C(CO)_{17}]^{2-}$, in the absence of cadmium halide salts, gives rise to formation of $[H_{6-n}Ni_{34}C_4(CO)_{34}]^{n-}$ ($n=4$, 5) clusters in good yields.

$$4\,[Ni_9C(CO)_{17}]^{2-} + 4\,H^+ \rightarrow [H_2Ni_{34}C_4(CO)_{38}]^{4-} + 22\,CO + H_2 + 2\,Ni(CO)_4 \quad (2)$$

The function of the $[CdCl]^+$ moieties therefore, seems to be to intercept the intermediate $Ni_{30}C_4$ moiety, by capping its two pentagonal faces.

The same $[H_{6-n}Ni_{30}C_4(CO)_{34}(CdCl)_2]^{n-}$ ($n=3$–6) species can be obtained, even though in lower yields, from the reaction of $CdCl_2{\cdot}2.5\,H_2O$ with $[Ni_{10}C_2(CO)_{16}]^{2-}$ or $[Ni_{16}C_4(CO)_{23}]^{4-}$, whose intermediate formation in Equation (2) has been detected experimentally by IR monitoring.

X-ray structures of $[NMe_3(CH_2Ph)]_4[H_2Ni_{30}C_4(CO)_{34}(CdCl)_2]{\cdot}2\,COMe_2$, $[NEt_4]_5[HNi_{30}C_4(CO)_{34}(CdCl)_2]{\cdot}2\,MeCN$, and $[NMe_4]_6[Ni_{30}C_4(CO)_{34}(CdCl)_2]{\cdot}6\,MeCN$: The molecular structures of $[H_2Ni_{30}C_4(CO)_{34}(CdCl)_2]^{4-}$, $[HNi_{30}C_4(CO)_{34}(CdCl)_2]^{5-}$, and $[Ni_{30}C_4(CO)_{34}(CdCl)_2]^{6-}$ are almost identical; only that of $[H_2Ni_{30}C_4(CO)_{34}(CdCl)_2]^{4-}$ is reported in Figure 2. However, the average bond lengths of all the species are compared with those of $[HNi_{34}C_4(CO)_{38}]^{5-}$ and $[Ni_{35}C_4(CO)_{39}]^{6-}$ in Table 1. Full lists of the individual bond lengths are given in the Supporting Information. The structures of the $[H_{6-n}Ni_{30}C_4(CO)_{34}(CdCl)_2]^{n-}$ ($n=4$–6) can be thought as composed of the carbide carbonyl cluster $[H_{6-n}Ni_{30}C_4(CO)_{34}]^{(n+2)-}$ intercepted by two $[CdCl]^+$ moieties. The nickel tetracarbide core of these clusters is strictly related to that reported previously for $[HNi_{34}C_4(CO)_{38}]^{5-}$ and $[Ni_{35}C_4(CO)_{39}]^{6-}$.[14]

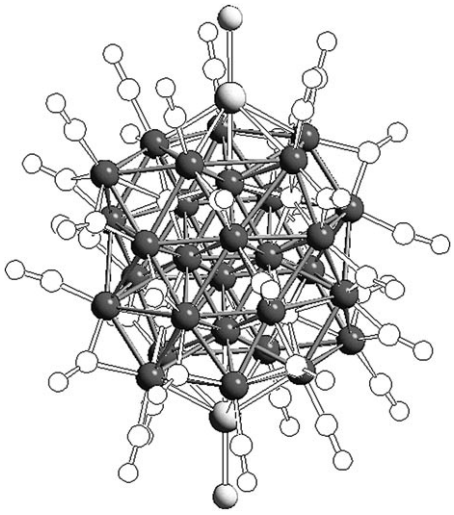

Figure 2. Molecular structure of $[H_2Ni_{30}C_4(CO)_{34}(CdCl)_2]^{4-}$ (dark gray: nickel; lightly shaded: cadmium and chlorine).

For clarity, the formal build-up of the nickel carbide frame of all five clusters is represented in Figure 3. They are composed of a Ni_{20} cubic close-packed (CCP) core (**A**), which has 28 triangular and four square faces on its surface. The four carbide atoms are located over these square faces (**B**), and a trigonal prismatic cage can be obtained around each of them by condensing two more Ni atoms over these faces, resulting in a $Ni_{28}C_4$ fragment (**C**). This moiety shows 38 triangular, four square, and two pentagonal faces, and two more Ni atoms can be added onto two of the opposite square faces, to give a $Ni_{30}C_4$ fragment (**D**). Now, if the two pentagonal faces are blocked by two $CdCl^+$ moieties, then the $Ni_{30}C_4(CdCl)_2$ core of $[H_{6-n}Ni_{30}C_4(CO)_{34}(CdCl)_2]^{n-}$ is obtained (**E**). Conversely, if the two pentagonal faces are each capped by one Ni(CO) moiety (isoelectronic with $[CdCl]^+$),

Table 1. Average bond lengths in $[H_2Ni_{30}C_4(CO)_{34}(CdCl)_2]^{4-}$, $[HNi_{30}C_4(CO)_{34}(CdCl)_2]^{5-}$, $[Ni_{30}C_4(CO)_{34}(CdCl)_2]^{6-}$, $[HNi_{34}C_4(CO)_{38}]^{5-}$, and $[Ni_{35}C_4(CO)_{39}]^{6-}$.

	$[H_2Ni_{30}C_4(CO)_{34}(CdCl)_2]^{4-}$	$[HNi_{30}C_4(CO)_{34}(CdCl)_2]^{5-}$	$[Ni_{30}C_4(CO)_{34}(CdCl)_2]^{6-}$	$[HNi_{34}C_4(CO)_{38}]^{5-}$	$[Ni_{35}C_4(CO)_{39}]^{6-}$
Ni–Ni, all	2.593	2.596	2.599	2.597	2.596
Ni–Ni, CCP[a]	2.579	2.585	2.585	2.571	2.568
Ni–C(6)[b]	1.94	1.95	1.92	1.94	1.94
Ni–C(7)[c]	2.01	2.01	2.02	2.01	2.03
Ni–Cd	2.764	2.768	2.757	–	–
Cd–Cl	2.381	2.421	2.446	–	–

[a] Average Ni–Ni distance in the CCP Ni_{20} core (see text for descriptions of the structures). [b] Average Ni–C distance in the trigonal prismatic cavities. [c] Average Ni–C distance in the capped trigonal prismatic cavities.

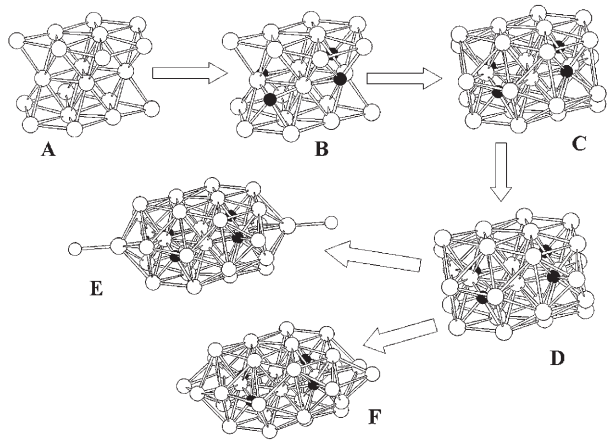

Figure 3. Formal growth path of the metal cores of $[H_{6-n}Ni_{30}C_4(CO)_{34}(CdCl)_2]^{n-}$ and $[HNi_{34}C_4(CO)_{38}]^{5-}$: **A**) Ni_{20} CCP core; **B**) $Ni_{20}C_4$; **C**) $Ni_{28}C_4$ with the four carbide atoms in trigonal prismatic cages; **D**) $Ni_{30}C_4$ after capping of two opposite trigonal prismatic cages; **E**) the $Ni_{30}C_4(CdCl)_2$ core of $[H_{6-n}Ni_{30}C_4(CO)_{34}(CdCl)_2]^{n-}$; **F**) the $Ni_{34}C_4$ core of $[HNi_{34}C_4(CO)_{38}]^{5-}$.

and then further Ni(CO) moieties (addition of which does not alter the number of cluster valence electrons) are added on the resulting butterfly faces, then the metal core of $Ni_{32+x}C_4(CO)_{36+x}$ ($x=1$, 2, 3, etc.) species would be formed (**F**). Of these, the structures of $[HNi_{34}C_4(CO)_{38}]^{5-}$ ($x=2$) and $[Ni_{35}C_4(CO)_{39}]^{6-}$ ($x=3$) have already been documented.[14]

In these two series of clusters, the four carbide atoms occupy, two by two, two different types of trigonal prismatic cavities. Thus, two carbides are found in almost regular trigonal prismatic cages (Ni–C_{av} = 1.92–1.95 Å), whereas the other two are inside distorted capped trigonal prismatic cavities, displaying seven metal–carbide interactions (Ni–C_{av} = 2.01–2.03 Å). The apparent radii for the carbide carbons are 0.63–0.66 and 0.73–0.75 Å, respectively. These values as well as the average Ni–Ni distances (see Table 1) for the five species are identical within experimental error, suggesting negligible effects on the $Ni_{30}C_4$ core following addition of $[CdCl]^+$ or Ni(CO) fragments and/or changes in the cluster anionic charge. The resulting metallic frames originate in the fusion of a CCP chunk of Ni atoms with hexagonal, pentagonal-bipyramidal, and tetrahedral fragments. This structure is the result of the disturbing action exerted on the nickel close-packed lattice by the presence of carbide atoms, which cannot shrink into octahedral cavities that are too small. An analogous effect has been proved previously in other nickel carbide clusters such as $[Ni_7C(CO)_{12}]^{2-}$,[12] $[Ni_8C(CO)_{16}]^{2-}$, $[Ni_9C(CO)_{17}]^{2-}$,[13] $[H_{6-n}Ni_{38}C_6(CO)_{42}]^{n-}$, and $[H_{6-n}Ni_{32}C_6(CO)_{36}]^{n-}$.[15,16] Thus, the carbide atom was found in a capped trigonal-prismatic cavity in $[Ni_7C(CO)_{12}]^{2-}$, whereas it was lodged in square-antiprismatic cavities for all the other clusters.

The structures of the $[H_{6-n}Ni_{30}C_4(CO)_{34}(CdCl)_2]^{n-}$ anions are completed by 34 Ni-bonded carbonyl ligands, 14 of which are terminal and 20 edge-bridging, and two chloride ligands bonded to the Cd atoms. Only minor differences in the stereochemistry of the carbonyl ligands exist between the three species, since some of the terminal CO groups might have incipient edge-bridging character and, similarly, some of the edge-bridging carbonyls might display incipient face-bridging behavior.

Even though the $[H_{6-n}Ni_{30}C_4(CO)_{34}(CdCl)_2]^{n-}$ ($n=4$–6), $[HNi_{34}C_4(CO)_{38}]^{5-}$, and $[Ni_{35}C_4(CO)_{39}]^{6-}$ carbido clusters are structurally very closely related, they are not isoelectronic. The Ni–Cd carbido derivatives formally display $12n+32$ cluster valence electrons, whereas the homometallic nickel carbides only feature $12n+30$ valence electrons. This observation prompted parallel electrochemical studies of the two series of compounds and an extended Hückel molecular orbital (EHMO) analysis; the results are reported in the next two sections respectively.

Electrochemical studies of $[H_{6-n}Ni_{30}C_4(CO)_{34}(CdCl)_2]^{n-}$ and $[Ni_{34}C_4(CO)_{38}]^{6-}$: The limited solubility of all the salts of the title anions in the presence of supporting electrolytes and the protonation–deprotonation equilibria illustrated in Scheme 1 make electrochemical investigations of $[H_{6-n}Ni_{30}C_4(CO)_{34}(CdCl)_2]^{n-}$ rather troublesome. Depending on the solvent, more or less protonated $[H_{6-n}Ni_{30}C_4(CO)_{34}(CdCl)_2]^{n-}$ species exist concomitantly in solution. This gives rise to weakly separated electron-transfer processes, typically exemplified by the voltammetric responses given by $[H_2Ni_{30}C_4(CO)_{34}(CdCl)_2]^{4-}$ in MeCN (Figure 4).

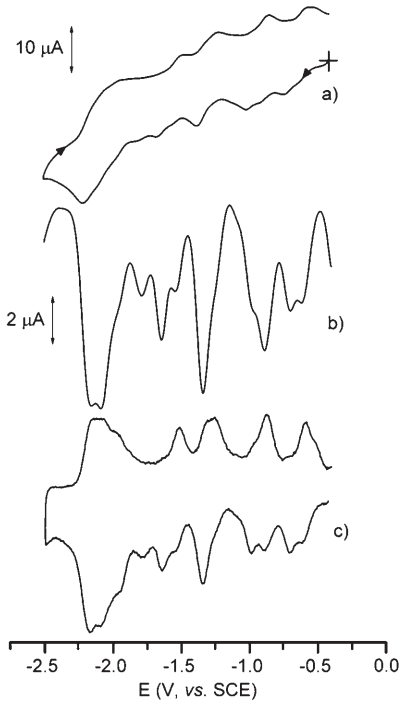

Figure 4. Voltammetric profiles recorded at a mercury electrode of $[NEt_4]_4[H_2Ni_{30}C_4(CO)_{34}(CdCl)_2]$ in MeCN (saturated solution); supporting electrolyte $[NEt_4][PF_6]$ (0.1 mol dm^{-3}). a) Cyclic voltammetry; b) Osteryoung square-wave voltammetry; c) first derivative deconvoluted voltammetry. Scan rates: a) 0.2 V s^{-1}; b) 0.1 V s^{-1}.

As shown, simply limiting ourselves to the first three main reduction processes possessing features of chemical reversibility in the short times of cyclic voltammetry and naively assigned to the sequence $[H_2Ni_{30}C_4(CO)_{34}(CdCl)_2]^{4-/5-/6-/7-}$, each process is split into two closely spaced peaks (as is quite evident from the mathematical treatment in Figure 4c). Even if the $[H_2Ni_{30}C_4(CO)_{34}(CdCl)_2]^{4-}/[HNi_{30}C_4(CO)_{34}(CdCl)_2]^{5-}$ equilibrium is shifted toward the penta-anion in acetonitrile, significant amounts of the tetra-anion are probably still present, which make assignment of the different steps impossible. In contrast, a more precise voltammetric picture is exhibited by the completely deprotonated $[Ni_{30}C_4(CO)_{34}(CdCl)_2]^{6-}$ hexa-anion in DMF (Figure 5).

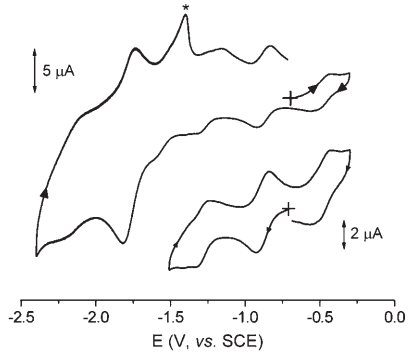

Figure 5. Cyclic voltammetric profiles recorded at a mercury electrode of $[NEt_4]_6[Ni_{30}C_4(CO)_{34}(CdCl)_2]$ in DMF (0.8×10^{-3} mol dm^{-3}); supporting electrolyte $[NEt_4][PF_6]$ (0.1 mol dm^{-3}), scan rate 0.2 V s^{-1}.

As shown, it exhibits both an oxidation ($E^{o\prime}_{6-/5-}=-0.49$ V *vs.* SCE) and two well separated reductions ($E^{o\prime}_{6-/7-}=-0.88$ V; $E^{o\prime}_{7-/8-}=-1.28$ V), all of which display features of chemical reversibility. A further reduction process ($E^{o\prime}=-1.78$ V) with a markedly higher peak is also present which in the reverse scan shows a stripping anodic peak (the asterisked peak in the figure), which increases with a decrease in the scan rate. Based on such a feature, we assign this cathodic process to the partially chemically reversible Cd-centered step $[Ni_{30}C_4(CO)_{34}(CdCl)_2]^{8-/10-}$, followed by release of Cd metal. This picture now makes the previous voltammetric profile of $[H_2Ni_{30}C_4(CO)_{34}(CdCl)_2]^{4-}$ a little more comprehensible. In fact, in that case also a higher-current process is present at quite negative potential values ($E^{o\prime}\approx-2.1$ V).

The different voltammetric responses of the anions $[H_{6-n}Ni_{30}C_4(CO)_{34}(CdCl)_2]^{n-}$ ($n=4$–6) are in keeping with the presence of hydride atoms, at least in the less charged penta- and tetra-anions. Otherwise, overlapping steady-state profiles would have been observed for $n=4$, 5, and 6. This is also in agreement with the fact that the formation of the species with $n=3$–5 is observed only by addition of acids and not by employing mild oxidizing agents (see the section on synthesis and characterization of $[H_{6-n}Ni_{30}C_4(CO)_{34}(CdCl)_2]^{n-}$ ($n=3$–6) clusters, above). Further circumstantial indirect evidence for the presence of hydride atoms is provided by a comparison between the electrochemical and the chemical behavior of $[Ni_{30}C_4(CO)_{34}(CdCl)_2]^{6-}$ upon addition of protonic acids (see Scheme 1). Indeed, while electrochemical oxidation generates the $[Ni_{30}C_4(CO)_{34}(CdCl)_2]^{6-/5-}$ redox couple as the only redox change with features of complete chemical reversibility at a high scan rate, protonation of $[Ni_{30}C_4(CO)_{34}(CdCl)_2]^{6-}$ reversibly and sequentially neutralizes the charge up to the trianion. Besides, the penta- and tetra-anions are stable enough to be isolated and crystallized. Therefore, their complete formula should be $[H_{6-n}Ni_{30}C_4(CO)_{34}(CdCl)_2]^{n-}$ ($n=4$, 5).

The electrochemical behavior of the structurally related $[Ni_{34}C_4(CO)_{38}]^{6-}$ hexa-anion (Figure 6) is even more conclusive. It exhibits three reversible reductions ($E^{o\prime}_{6-/7-}=-1.21$ V; $E^{o\prime}_{7-/8-}=-1.38$ V; $E^{o\prime}_{8-/9-}=-1.85$ V). Three irreversible oxidations (not shown in Figure 6) are also present at positive potentials. Because of the limited solubility of the sample, the reduction steps are not well defined in the cyclic voltammetry, but they appear better resolved in deconvolutive voltammetry. Significantly, the markedly higher reduction process present in the voltammetric profile of $[H_{6-n}Ni_{30}C_4(CO)_{34}(CdCl)_2]^{n-}$, accompanied in the reverse scan by a stripping anodic peak, is no longer present. This further validates the assignment of this latter process as a Cd-centered redox step.

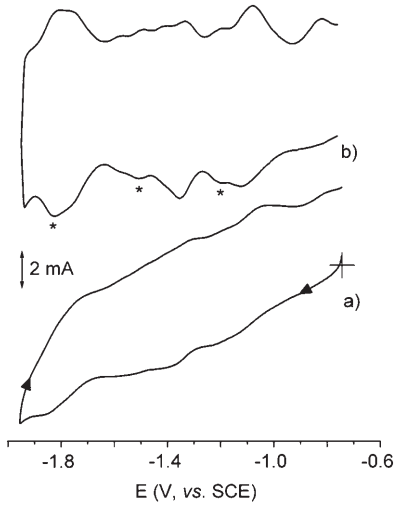

Figure 6. Cathodic voltammetric profiles recorded at a Pt electrode of $[NEt_4]_6[Ni_{34}C_4(CO)_{38}]$ in MeCN (saturated solution); supporting electrolyte $[NEt_4][PF_6]$ (0.1 mol dm^{-3}). a) Cyclic and b) first-derivative deconvoluted voltammetry; scan rates 0.2 V s^{-1}.

Cyclic voltammetric profiles of $[H_{6-n}Ni_{34}C_4(CO)_{38}]^{n-}$ ($n=4$, 5) salts were even less resolved, probably owing to additional complications arising from protonation–deprotonation equilibria, as for the $[H_{6-n}Ni_{30}C_4(CO)_{34}(CdCl)_2]^{n-}$ ($n=4$, 5) species. Residual traces of such protonated species (asterisked peaks) seem to be responsible for the splitting of the cathodic processes illustrated in Figure 6. Once again, the lack of any reversible oxidation step in the electrochemical oxidation of $[Ni_{34}C_4(CO)_{38}]^{6-}$ and the fact that the purported

$[H_{6-n}Ni_{34}C_4(CO)_{38}]^{n-}$ ($n=4$, 5) can be isolated by protonation of the hexa-anion strongly support the presence of hydrides in the latter less-charged ($n=4$, 5) species.

EHMO analysis of $[H_{6-n}Ni_{30}C_4(CO)_{34}(CdCl)_2]^{n-}$ (n=4–6) and $[Ni_{34}C_4(CO)_{38}]^{6-}$: Extended Hückel molecular orbital (EHMO) analysis of $[H_{6-n}Ni_{30}C_4(CO)_{34}(CdCl)_2]^{n-}$ ($n=4$–6) and $[Ni_{34}C_4(CO)_{38}]^{6-}$, using their crystallographic coordinates, has been carried out with CACAO,[32] to explain the differences in their numbers of cluster valence electrons. The calculations were performed by combining the molecular orbitals of a $[Ni_{30}C_4(CO)_{34}]^{n-}$ ($n=8$ and 6, respectively) fragment with those of two outer $CdCl^+$ or $Ni_2(CO)_2$ fragments. The frontier regions (in the −11.2 to −9.3 eV energy interval) of the EHMO diagrams of $[Ni_{34}C_4(CO)_{38}]^{6-}$ and $[Ni_{30}C_4(CO)_{34}(CdCl)_2]^{6-}$ are compared in the two diagrams in Figure 7, which indicate that there are 18 and 17 closely

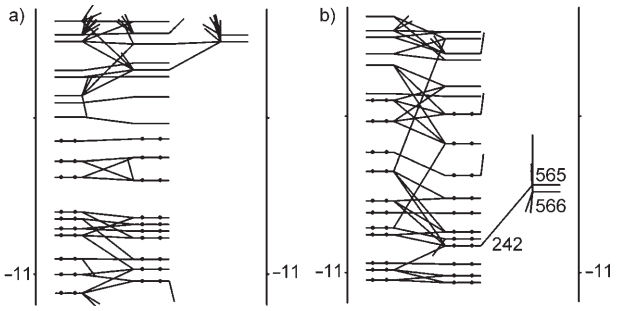

Figure 7. Frontier regions (in the −11.2 to −9.3 eV energy interval) of the EHMO diagrams of a) $[Ni_{34}C_4(CO)_{38}]^{6-}$ and b) $[Ni_{30}C_4(CO)_{34}(CdCl)_2]^{6-}$.

spaced MOs respectively in an energy interval of less than 2 eV, and a well defined HOMO–LUMO gap can hardly be identified. The energy levels of the two slightly different $[Ni_{30}C_4(CO)_{34}]^{n-}$ core fragments (on the left in each diagram) are very similar. The first and second LUMOs (566 and 565, respectively, in Figure 7b) of the $[Cl{-}Cd{\cdots}CdCl]^{2+}$ fragment are approximately 1 eV lower in energy then the corresponding first and second LUMOs of the $[(CO)_2Ni_2{\cdots}Ni_2(CO)_2]$ fragment and are degenerate. These fragment molecular orbitals of the $[Cl{-}Cd{\cdots}CdCl]^{2+}$ moiety are shown pictorially in Figure 8. The major differences between the EHMO diagrams of $[Ni_{34}C_4(CO)_{38}]^{6-}$ and $[Ni_{30}C_4(CO)_{34}(CdCl)_2]^{6-}$ (in the center of each diagram) arise from the weak interaction of the LUMO orbitals of the $[Cl{-}Cd{\cdots}CdCl]^{2+}$ moiety with the antibonding orbitals of suitable symmetry of the $[Ni_{30}C_4(CO)_{34}]^{8-}$ fragment. This generates the filled, weakly stabilized molecular orbital 242 (at the eighth energy level down from the HOMO) in the $[Ni_{30}C_4(CO)_{34}(CdCl)_2]^{6-}$ diagram; this cluster valence orbital (CVO) is represented in Figure 9.

In contrast, owing to the higher energy of the LUMO orbitals of the $[(CO)_2Ni_2{\cdots}Ni_2(CO)_2]$ fragment, their weak interactions with antibonding orbitals of suitable symmetry of the $[Ni_{30}C_4(CO)_{34}]^{6-}$ fragment only increases the multitude

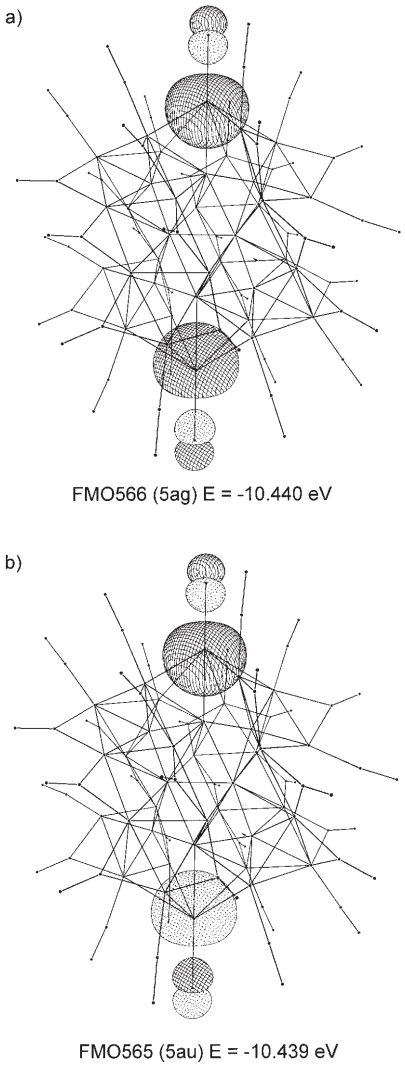

Figure 8. a) First and b) second LUMOs of the $[Cl{-}Cd{\cdots}CdCl]^{2+}$ fragment.

of empty antibonding energy levels of $[Ni_{34}C_4(CO)_{38}]^{6-}$. Therefore, according to EHMO calculations, $[Ni_{34}C_4(CO)_{38}]^{6-}$ should display one fewer filled CVO than $[Ni_{30}C_4(CO)_{34}(CdCl)_2]^{6-}$, as is found experimentally.

Finally, the presence of several low-lying empty orbitals and the absence of a well defined gap in both diagrams in Figure 7 are in keeping with the electrochemical behavior of both series of compounds described in the previous section.

Conclusion

It has been found that the weak acidity of $CdCl_2{\cdot}2.5\,H_2O$ allows fairly selective syntheses of higher-nuclearity clusters on starting from preformed lower-nuclearity anionic carbonyl clusters. Its reaction with $[Rh_7(CO)_{16}]^{3-}$ has been shown to lead to $[Rh_{15}(CO)_{27}]^{3-}$ and $[Rh_{17}(CO)_{30}]^{3-}$ homometallic species, which do not include Cd moieties in their metal frames.[26] In contrast, its reaction with $[Ni_9C(CO)_{17}]^{2-}$ re-

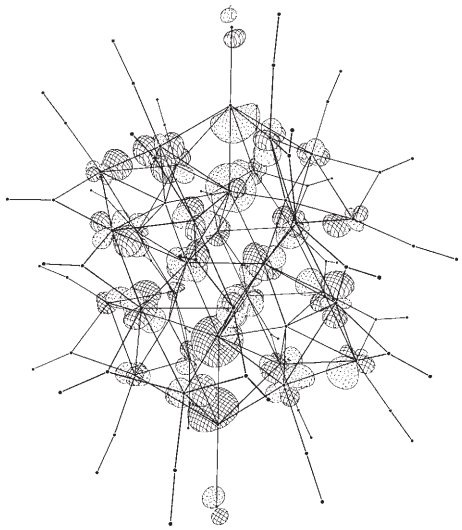

Figure 9. Pictorial representation of CVO 242 ($E=-10.820$ eV) for $[Ni_{30}C_4(CO)_{34}(CdCl)_2]^{6-}$ (the contributions of the atomic orbitals of C and O are omitted for clarity).

sults in new high-nuclearity heterometallic nickel carbide carbonyl clusters with $[CdCl]^+$ moieties associated in their structures, $[H_{6-n}Ni_{30}C_4(CO)_{34}(CdCl)_2]^{n-}$ ($n=3$–6). Three of these anions bearing different charges ($n=4$–6) have been structurally characterized, and exhibit almost identical geometries and bonding parameters. The fact that their structures are closely related to those reported previously for the $[HNi_{34}C_4(CO)_{38}]^{5-}$ and $[Ni_{35}C_4(CO)_{39}]^{6-}$ species seems to imply that the stepwise assembly of their nickel carbide cores, originally suggested only with the purpose of introducing their structures step-by-step,[14] is a more general formal growth path for nickel tetracarbide clusters. Moreover, it may be hoped that the interception of $Ni_{30}C_4(CO)_{34}$ fragments by $[CdCl]^+$ moieties will open additional possibilities for their interception with other moieties and provide possible sites to connect the resulting clusters in 1D chains assembled by alternation of molecular capacitors with conducting spacers, as already reported recently for the $[Ni_{12}(CO)_{24}(Cd_2Cl_3)]^{3-}$ dimer[33] or the $[Pt_9(CO)_{18}(CdCl_2)_2]^{2-}$ infinite chains.[34]

The quite complex metal motifs of these metal clusters, which are the result of growing noncompact Ni_6C and Ni_7C trigonal prismatic units around a compact Ni core, may represent snapshots of the deformation that a compact first-row metal particle would undergo upon incorporation of carbon atoms, as occurs in methanation reactions and in the production of carbon nanotubes. Apart from other considerations, as illustrated by step **D** of Figure 3 the deformations brought about by lodging carbide atoms within a Ni particle give rise to concave bis-triangular faces on the cluster surface, which may resemble step defects on top of a metal surface. Such step defects have been suggested as the active sites for the activation of several C_1 and C_2 molecules.[35] For instance, dual coordination of CO within the wings of a butterfly cluster (for example, $[HFe_4(CO)_{12}(\mu_4\text{-}\eta^2\text{-}CO)]^-$[36]) has been demonstrated to undergo proton-induced C–O bond cleavage and reduction to CH_4.[37]

We also believe we have confirmed that electrochemical studies, as well as disclosing the nanocapacitor behavior of molecular clusters, when analyzed in conjunction with chemical reactivity studies, can also provide unambiguous though only circumstantial evidence for the presence of hydrides, which elude direct detection by ^{1}H NMR spectroscopy. At present, we do not have explanations for our failure to detect ^{1}H NMR signals of hydrides in high-nuclearity clusters and its interpretation should be postponed.

The chemistry of transition metal/main group heteroatoms represents an emerging field with potential impact in the nanosciences (as heterometallic nanoparticles), catalysis (deposited on high surface area materials), composite materials (grafted on surfaces or self-assembled), and metallurgy (as precursors to metastable alloys).[2] Finally, any further improvement of the reversible redox properties of these high-nuclearity metal clusters, which are already nanomaterials as judged by dimensions and have the advantage over monodispersed ligand-stabilized metal nanoparticles of displaying constant composition and geometry, will make them increasingly interesting as nanocapacitors for assembly of molecular devices for molecular electronics.

Experimental Section

General: All reactions and sample manipulations were carried out using standard Schlenk techniques under nitrogen and in dried solvents. All the reagents were commercial products (Aldrich) of the highest purity available and used as received. The $[NR_4]_2[Ni_9C(CO)_{17}]$ (NR_4=NEt_4, NMe_4, $NMe_3(CH_2Ph)$),[13] $[NMe_4]_2[Ni_{10}C_2(CO)_{16}]$,[17] and $[NMe_4]_4[Ni_{16}C_4(CO_{23}]$[18] salts have been prepared according to the literature. Ni and Cd were analyzed by atomic absorption on a Pye–Unicam instrument. C,H,N analyses were obtained with a ThermoQuest FlashEA 1112NC instrument. IR spectra were recorded on a Perkin–Elmer SpectrumOne interferometer in CaF_2 cells. ESI mass spectra were recorded on a Waters Micromass ZQ4000 instrument. All NMR measurements were performed on Varian Inova 600 and Mercury Plus 400 instruments. Cyclic voltammetry was performed in a three-electrode cell containing a platinum working electrode surrounded by a platinum-spiral counter electrode, and an aqueous saturated calomel reference electrode (SCE) mounted with a Luggin capillary. A BAS 100 W electrochemical analyzer was used as polarizing unit. All the potential values are referred to the SCE. Under the present experimental conditions, the one-electron oxidation of ferrocene occurs at $E^{o\prime}=+0.59$ V in THF. Controlled potential coulometry was performed in an H-shaped cell with anodic and cathodic compartments separated by a sintered-glass disk. The working macroelectrode was a platinum gauze; a mercury pool was used as the counter electrode. Structure drawings have been performed with SCHAKAL99.[38]

Synthesis of $[NMe_3(CH_2Ph)]_4[H_2Ni_{30}C_4(CO)_{34}(CdCl)_2]\cdot 2COMe_2$: $CdCl_2\cdot 2.5\,H_2O$ (0.470 g, 2.06 mmol) was added in portions to a solution of $[NMe_3(CH_2Ph)]_2[Ni_9C(CO)_{17}]$ (2.01 g, 1.54 mmol) in THF (30 mL) with stirring. The mixture was left to react for 3 h, until all the starting $[NMe_3(CH_2Ph)]_2[Ni_9C(CO)_{17}]$ had disappeared according to IR monitoring. The resulting dark brown suspension was evaporated to dryness. The residue was washed with water (40 mL) and THF (30 mL) to remove all Ni^{II} and Cd^{II} salts and minor quantities of lower-nuclearity nickel carbide carbonyl clusters. Extraction in acetone (30 mL) resulted in a dark brown solution of the target compound. Precipitation by slow diffusion of *i*PrOH

(60 mL) gave a dark brown crystalline precipitate of $[NMe_3(CH_2Ph)]_4[H_2Ni_{30}C_4(CO)_{34}(CdCl)_2]\cdot 2\,COMe_2$ (yield 1.15 g, 66.0% based on Ni). The salt is soluble in acetone, acetonitrile, DMF, and DMSO, sparingly soluble in THF and alcohols, and insoluble in nonpolar solvents.

$C_{84}H_{76}Cd_2Cl_2N_4Ni_{30}O_{36}$: IR (acetone, 293 K): 2019 (s), 1874 (m) cm^{-1}; elemental analysis (%): calcd. for $C_{84}H_{76}Cd_2Cl_2N_4Ni_{30}O_{36}$ (3774.04): C 26.73, H 2.03, N 1.48, Ni 46.66, Cd 5.96; found: C 26.92, H 1.89, N 1.55, Ni 46.42, Cd 6.03.

Other salts of this tetra-anion, $[NR_4]_4[H_2Ni_{30}C_4(CO)_{34}(CdCl)_2]$ [NR_4 = NMe_4, NEt_4, NBu_4], can be obtained by the same procedure as above, employing the relevant $[NR_4]_2[Ni_9C(CO)_{17}]$ salts. The same products can be obtained, even if in lower yields, from the reaction of $[Ni_{10}C_2(CO)_{16}]^{2-}$ or $[Ni_{16}C_4(CO)_{23}]^{4-}$ with $CdCl_2\cdot 2.5\,H_2O$ in THF or acetone.

Synthesis of $[NEt_4]_5[HNi_{30}C_4(CO)_{34}(CdCl)_2]\cdot 2\,MeCN$: $CdCl_2\cdot 2.5\,H_2O$ (0.558 g, 2.44 mmol) was added in portions to a solution of $[NEt_4]_2[Ni_9C(CO)_{17}]$ (2.25 g, 1.78 mmol) in THF (30 mL) with stirring. Reaction of this mixture, evaporation to dryness, and washing of the residue were similar to the procedures described above. Extraction into acetonitrile (30 mL) resulted in a dark brown solution of the target compound. Precipitation by slow diffusion of diisopropyl ether (60 mL) gave a dark brown crystalline precipitate of $[NEt_4]_5[HNi_{30}C_4(CO)_{34}(CdCl)_2]\cdot 2\,MeCN$ (yield 1.31 g, 64.7% based on Ni). The salt is soluble in acetonitrile, DMF, and DMSO, sparingly soluble in acetone, and insoluble in less polar solvents.

$C_{82}H_{106}Cd_2Cl_2N_7Ni_{30}O_{34}$: IR (acetonitrile, 293 K): 2008 (s), 1862 (m) cm^{-1}; elemental analysis (%): calcd. for $C_{82}H_{106}Cd_2Cl_2N_7Ni_{30}O_{34}$ (3790.28): C 25.98, H 2.82, N 2.59, Ni 46.46, Cd 5.93; found: C 26.09, H 2.95, N 2.37, Ni 46.58, Cd 5.88.

Synthesis of $[NMe_4]_6[Ni_{30}C_4(CO)_{34}(CdCl)_2]\cdot 6\,MeCN$: A solution of $[NMe_4]_5[HNi_{30}C_4(CO)_{34}(CdCl)_2]$ in acetonitrile was prepared by a procedure similar to that reported above. Thus, $CdCl_2\cdot 2.5\,H_2O$ (0.558 g, 2.44 mmol) was added in portions to a solution of $[NMe_4]_2[Ni_9C(CO)_{17}]$ (2.12 g, 1.84 mmol) in acetone (30 mL) with stirring. Reaction of this mixture, evaporation to dryness, and washing of the residue were similar to the procedures described above. After extraction in acetonitrile (30 mL), 4,4′-bipyridine (0.35 g, 2.24 mmol) was added to the residue and the solution was stirred overnight. The IR spectrum at this point showed ν(CO) at 2003 (s), 1995 (sh), 1856 (br) cm^{-1}, as expected for a mixture of $[HNi_{30}C_4(CO)_{34}(CdCl)_2]^{5-}$ and $[Ni_{30}C_4(CO)_{34}(CdCl)_2]^{6-}$. This mixture was filtered to remove all solids. Precipitation by slow diffusion of diisopropyl ether (60 mL) gave a dark brown crystalline precipitate of $[NMe_4]_6[Ni_{30}C_4(CO)_{34}(CdCl)_2]\cdot 6\,MeCN$ (yield 0.868 g, 42.0% based on Ni). The salt is soluble in acetonitrile, DMF, and DMSO, sparingly soluble in acetone, and insoluble in less polar solvents.

$C_{74}H_{90}Cd_2Cl_2N_{12}Ni_{30}O_{34}$: IR (DMF, 293 K): 1996 (s), 1855 (m) cm^{-1}; elemental analysis (%): calcd. for $C_{74}H_{90}Cd_2Cl_2N_{12}Ni_{30}O_{34}$: (3748.58): C 23.71, H 2.42, N 4.48, Ni 46.98, Cd 6.00; found: C 23.96, H 2.55, N 4.21, Ni 46.49, Cd 6.15.

X-ray crystallographic study: Crystal data and collection details for $[NMe_3(CH_2Ph)]_4[H_2Ni_{30}C_4(CO)_{34}(CdCl)_2]\cdot 2\,COMe_2$, $[NEt_4]_5[HNi_{30}C_4(CO)_{34}(CdCl)_2]\cdot 2\,MeCN$ and $[NMe_4]_6[Ni_{30}C_4(CO)_{34}(CdCl)_2]\cdot 6\,MeCN$ are reported in Table 2. The diffraction experiments were carried out on a Bruker APEX II diffractometer equipped with a CCD detector using $Mo_{K\alpha}$ radiation. Data were corrected for Lorentz polarization and absorption effects (empirical absorption correction by SADABS).[39] Structures were solved by direct methods and refined by full-matrix least-squares refinement based on all the data using F^2.[40] Hydrogen atoms were fixed at calculated positions and refined by a riding model. All non-hydrogen atoms were refined with anisotropic displacement parameters, unless otherwise stated. The asymmetric units for the three structures contain, respectively: half a cluster anion (located on an inversion center), two $[NMe_3(CH_2Ph)]^+$ ions, and one $COMe_2$ molecule for $[NMe_3$-

Table 2. Crystal data and experimental details for $[NMe_3(CH_2Ph)]_4[H_2Ni_{30}C_4(CO)_{34}(CdCl)_2]\cdot 2\,COMe_2$, $[NEt_4]_5[HNi_{30}C_4(CO)_{34}(CdCl)_2]\cdot 2\,MeCN$, and $[NMe_4]_6[Ni_{30}C_4(CO)_{34}(CdCl)_2]\cdot 6\,MeCN$.

	$[NMe_3(CH_2Ph)]_4[H_2Ni_{30}C_4(CO)_{34}(CdCl)_2]\cdot 2\,COMe_2$	$[NEt_4]_5[HNi_{30}C_4(CO)_{34}(CdCl)_2]\cdot 2\,MeCN$	$[NMe_4]_6[Ni_{30}C_4(CO)_{34}(CdCl)_2]\cdot 6\,MeCN$
formula	$C_{84}H_{76}Cd_2Cl_2N_4Ni_{30}O_{36}$	$C_{82}H_{106}Cd_2Cl_2N_7Ni_{30}O_{34}$	$C_{74}H_{90}Cd_2Cl_2N_{12}Ni_{30}O_{34}$
M_r	3774.49	3790.74	3748.58
T [K]	295(2)	295(2)	291(2)
λ [Å]	0.71073	0.71073	0.71073
crystal system	monoclinic	monoclinic	monoclinic
space group	$P2_1/n$	$C2/c$	$P2_1/n$
a [Å]	14.674(6)	20.3099(15)	14.819(2)
b [Å]	25.998(10)	23.5714(17)	25.099(4)
c [Å]	15.586(6)	24.9323(18)	15.347(2)
α [°]	90	90	90
β [°]	110.913(7)	96.6350(10)	94.374(2)
γ [°]	90	90	90
V [Å^3]	5554(4)	11856.0(15)	5691.8(15)
Z	2	4	2
ρ_{calcd} [g cm^{-3}]	2.257	2.124	2.187
μ [mm^{-1}]	5.440	5.097	5.308
F(000)	3732	7556	3720
crystal size [mm]	$0.21\times 0.18\times 0.12$	$0.22\times 0.16\times 0.13$	$0.22\times 0.16\times 0.13$
θ limits [°]	1.57–25.03	1.50–25.03	1.56–27.00
index ranges	$-17\le h\le 17$ $-30\le k\le 30$ $-18\le l\le 18$	$-24\le h\le 24$ $-28\le k\le 28$ $-29\le l\le 29$	$-18\le h\le 18$ $-32\le k\le 32$ $-19\le l\le 19$
reflections collected	52997	56121	62138
independent reflections	9829 [R_{int} = 0.0948]	10465 [R_{int} = 0.0502]	12417 [R_{int} = 0.0680]
completeness to θ = 25.03° [%]	100	99.9	99.9
data/restraints/parameters	9829/568/712	10465/789/698	12417/75/649
goodness of fit on F^2	1.016	1.041	1.017
R_1 [$I>2\sigma(I)$]	0.0496	0.0509	0.0412
wR_2 (all data)	0.1345	0.1630	0.1186
largest diff. peak and hole [e Å^{-3}]	0.842/−1.730	1.561/−2.214	0.706/−1.147

$(CH_2Ph)]_4[H_2Ni_{30}C_4(CO)_{34}(CdCl)_2]\cdot 2\,COMe_2$; half a cluster anion (located on an inversion center), two and a half $[NEt_4]^+$ ions, and one MeCN molecule for $[NEt_4]_5[HNi_{30}C_4(CO)_{34}(CdCl)_2]\cdot 2\,MeCN$; half a cluster anion (located on an inversion center), three $[NMe_4]^+$ ions, and three MeCN molecules for $[NMe_4]_6[Ni_{30}C_4(CO)_{34}(CdCl)_2]\cdot 6\,MeCN$.

Two $[NEt_4]^+$ ions in $[NEt_4]_5[HNi_{30}C_4(CO)_{34}(CdCl)_2]\cdot 2\,MeCN$ are disordered, of which one is located on a general position and the other with the nitrogen on a twofold axis. The atoms of the former were split into two positions and refined using one occupancy parameter per disordered group, whereas in the latter case an occupancy factor of 0.5 was assigned to the independent image of the cation. All the disordered atoms have been refined isotropically except the N atoms, which were refined anisotropically. Restraints were applied to the C–N and C–C distances of the NEt_4^+ ions and MeCN molecules in order to obtain a satisfactory model.

In all three structures similar *U* restraints were applied to the C, N, and O atoms because of the presence of these light atoms together with several heavy atoms. For the same reason, rigid bond restraints were applied to the anions in $[NMe_3(CH_2Ph)]_4[H_2Ni_{30}C_4(CO)_{34}(CdCl)_2]\cdot 2\,COMe_2$ and $[NEt_4]_5[HNi_{30}C_4(CO)_{34}(CdCl)_2]\cdot 2\,MeCN$.

CCDC 654232, 654233, and 654234 contain the supplementary crystallographic data for this paper. These data can be obtained free of charge from The Cambridge Crystallographic Data Centre via www.ccdc.cam.ac.uk/data_request/cif.

Acknowledgements

We thank the University of Bologna and the University of Siena and MUR (PRIN2006) for funding.

[1] B. F. G. Johnson, C. M. Martin in *Metal Clusters in Chemistry* (Eds.: P. Braunstein, L. A. Oro, P. R. Raithby), Wiley-VCH, Weinheim, **1999**, pp. 877–912.
[2] J. M. Goicoechea, M. W. Hull, S. C. Sevov, *J. Am. Chem. Soc.* **2007**, *129*, 7885–7893.
[3] a) P. Nikolaev, M. J. Bronikowski, R. K. Bradley, F. Rohmund, D. T. Colbert, K. A. Smith, R. E. Smalley, *Chem. Phys. Lett.* **1999**, *313*, 91–97; b) W. Li, S. Xie, W. Liu, R. Zhao, Y. Zhang, W. Zhou, G. Wang, L. Qian, *J. Mater. Sci.* **1999**, *34*, 2745–2749; c) Z. P. Huang, D. Z. Wang, J. G. Wen, M. Sennett, H. Gibson, Z. F. Ren, *Appl. Phys. A* **2002**, *74*, 387–391; d) Y. Zhang, Y. Li, K. D. Wang, H. Dai, *Appl. Phys. A* **2002**, *74*, 325–328.
[4] C. Femoni, F. Kaswalder, M. C. Iapalucci, G. Longoni, Zacchini, *Coord. Chem. Rev.* **2006**, *250*, 1580–1604.
[5] a) B. T. Heaton, J. A. Iggo, I. S. Podkorytov, D. J. Smawfield, S. P. Tunik in *Metal Clusters in Chemistry* (Eds.: P. Braunstein, L. A. Oro, P. R. Raithby), Wiley-VCH, Weiheim, **1999**, pp. 960–1000; b) A. Fumagalli, R. D. Pergola in *Metal Clusters in Chemistry* (Eds.: P. Braunstein, L. A. Oro, P. R. Raithby), Wiley-VCH, Weinheim, **1999**, pp. 323–347.
[6] a) G. Longoni, C. Femoni, M. C. Iapalucci, P. Zanello in *Metal Clusters in Chemistry* (Eds.: P. Braunstein, L. A. Oro, P. R. Raithby), Wiley-VCH, Weinheim, **1999**, 1137–1158; b) G. Longoni, M. C. Iapalucci in *Clusters and Colloids* (Ed.: G. Schmid), Wiley-VCH, Weinheim, **1994**, pp. 91–177.
[7] a) K. Hughes, K. Wade, *Coord. Chem. Rev.* **2000**, *197*, 191–229; b) A. Sironi, *J. Chem. Soc., Dalton Trans.* **1993**, 173–178.
[8] a) R. B. King, *New J. Chem.* **1988**, *12*, 493–499; b) J. F. Halet, D. G. Evans, D. M. P. Mingos, *J. Am. Chem. Soc.* **1988**, *110*, 87–90.
[9] a) A. F. Masters, J. T. Meyer, *Polyhedron* **1995**, *14*, 339–365; b) J. K. Battie, A. F. Masters, J. T. Meyer, *Polyhedron* **1995**, *14*, 829–868.
[10] a) J. C. Calabrese, L. F. Dahl, A. Cavalieri, P. Chini, G. Longoni, S. Martinengo, *J. Am. Chem. Soc.* **1974**, *96*, 2616–2618; b) D. Braga, F. Grepioni, P. Milne, E. Parisini, *J. Am. Chem. Soc.* **1993**, *115*, 5115–5122.
[11] a) G. Longoni, P. Chini, A. Cavalieri, *Inorg. Chem.* **1976**, *15*, 3025–3029; b) A. Ceriotti, G. Longoni, M. Marchionna, *Inorg. Synth.* **1989**, *26*, 316–319; c) G. Longoni, P. Chini, L. D. Cower, L. F. Dahl, *J. Am. Chem. Soc.* **1975**, *97*, 5034–5036; d) G. Longoni, P. Chini, *Inorg. Chem.* **1976**, *15*, 3029–3031; e) D. A. Nagaki, L. D. Lower, G. Longoni, P. Chini, L. F. Dahl, *Organometallics* **1986**, *5*, 1764–1771; f) G. Longoni, B. T. Heaton, P. Chini, *J. Chem. Soc. Dalton Trans.* **1980**, 1537–1542.
[12] A. Ceriotti, G. Piro, G. Longoni, M. Manassero, N. Masciocchi, M. Sansoni, *New J. Chem.* **1988**, *12*, 501–503.
[13] A. Ceriotti, G. Longoni, M. Manassero, M. Perego, M. Sansoni, *Inorg. Chem.* **1985**, *24*, 117–120.
[14] A. Ceriotti, A. Fait, G. Longoni, G. Piro, L. Resconi, F. Demartin, M. Manassero, N. Masciocchi, M. Sansoni, *J. Am. Chem. Soc.* **1986**, *108*, 5370–5371.
[15] F. Calderoni, F. Demartin, F. Fabrizi de Biani, C. Femoni, M. C. Iapalucci, G. Longoni, P. Zanello, *Eur. J. Inorg. Chem.* **1999**, 663–671.
[16] A. Ceriotti, A. Fait, G. Longoni, G. Piro, F. Demartin, M. Manassero, N. Masciocchi, M. Sansoni, *J. Am. Chem. Soc.* **1986**, *108*, 8091–8092.
[17] A. Ceriotti, G. Longoni, L. Resconi, M. Manassero, N. Masciocchi, M. Sansoni, *J. Chem. Soc., Chem. Commun.* **1985**, 181–182.
[18] A. Ceriotti, G. Piro, G. Longoni, M. Manassero, L. Resconi, N. Masciocchi, M. Sansoni, *J. Chem. Soc., Chem. Commun.* **1985**, 1402–1403.
[19] a) A. F. Wells, *Structural Inorganic Chemistry*, Oxford Science Publications, Oxford, **1987**; b) *ASM Handbook, Vol. 3: Alloy Phase Diagrams*, ASM International, Materials Park, Ohio, **1992**, p. 2.112.
[20] Q. Xie, E. Perez-Cordero, L. Echegoyen, *J. Am. Chem. Soc.* **1992**, *114*, 3978–3980.
[21] R. S. Ingram, M. J. Hostetler, R. W. Murray, T. G. Schaaff, J. T. Khoury, R. L. Whetten, T. P. Bigioni, D. K. Guthrie, P. N. First, *J. Am. Chem. Soc.* **1997**, *119*, 9279–9280.
[22] J. F. Hicks, A. C. Templeton, S. Chen, K. M. Sheran, R. Jasti, R. W. Murray, J. Debord, T. G. Schaaff, R. L. Whetten, *Anal. Chem.* **1999**, *71*, 3703–3711.
[23] a) D. T. Miles, R. W. Murray, *Anal. Chem.* **2003**, *75*, 1251–1257; b) B. M. Quinn, P. Liljeroth, V. Ruiz, T. Laaksonen, K. Kontturi, *J. Am. Chem. Soc.* **2003**, *125*, 6644–6645.
[24] U. Simon in *Metal Clusters in Chemistry* (Eds.: P. Braunstein, L. A. Oro, P. R. Raithby), Wiley-VCH, Weinheim, **1999**, pp. 1342–1363.
[25] a) G. Schmid, Y.-P. Liu, M. Schumann, T. Raschke, C. Radehaus, *Nano Lett.* **2001**, *1*, 405–407; b) M. H. V. Werts, M. Lambert, J.-P. Bourgoin, M. Brust, *Nano Lett.* **2002**, *2*, 43–47.
[26] D. Collini, F. F. de Biani, S. Fedi, C. Femoni, F. Kaswalder, M. C. Iapalucci, G. Longoni, C. Tiozzo, S. Zacchini, P. Zanello, *Inorg. Chem.* **2007**, *46*, 7971–7981.
[27] a) F. Demartin, C. Femoni, M. C. Iapalucci, G. Longoni, P. Macchi, *Angew. Chem.* **1999**, *111*, 552–554; *Angew. Chem. Int. Ed.* **1999**, *38*, 531–533; b) F. Demartin, C. Femoni, M. C. Iapalucci, G. Longoni, P. Zanello, *J. Cluster Sci.* **2001**, *12*, 61–74.
[28] A. Ceriotti, F. Demartin, G. Longoni, M. Manassero, M. Marchionna, G. Piva, M. Sansoni, *Angew. Chem.* **1985**, *97*, 708–710; *Angew. Chem. Int. Ed. Engl.* **1985**, *24*, 697–698.
[29] J. L. Vidal, R. C. Schoening, J. M. Troup, *Inorg. Chem.* **1981**, *20*, 227–238.
[30] J. M. Bemis, L. F. Dahl, *J. Am. Chem. Soc.* **1997**, *119*, 4545.
[31] a) F. Dassenoy, K. Philippot, T. O. Ely, C. Amiens, P. Lecante, E. Snoeck, A. Mosset, M. J. Casanove, B. Chaudret. *New J. Chem.* **1998**, 703–711; b) A. Badia, W. Gao, S. Singh, L. Demers, L. Cuccia, L. Reven, *Langmuir* **1996**, *12*, 1262–1269.
[32] C. Mealli, D. M. Proserpio, M. Davide, *J. Chem. Educ.* **1990**, *67*, 399.
[33] C. Femoni, M. C. Iapalucci, G. Longoni, F. Ranuzzi, S. Zacchini, S. Fedi, P. Zanello, *Eur. J. Inorg. Chem.* **2007**, 4064–4070.
[34] C. Femoni, F. Kaswalder, M. C. Iapalucci, G. Longoni, S. Zacchini, *Chem. Commun.* **2006**, 2135–2137.
[35] E. L. Muetterties, T. N. Rhodin, E. Band, C. F. Brucker, W. R. Pretzen, *Chem. Rev.* **1979**, *79*, 91–137.

[36] a) W. Hieber, R. Werner, *Chem. Ber.* **1957**, *90*, 286–296; b) M. Manassero, M. Sansoni, G. Longoni, *J. Chem. Soc., Chem. Commun.* **1976**, 919–920.
[37] a) K. Whitmire, D. F. Shriver, *J. Am. Chem. Soc.* **1980**, *102*, 1456–1457; b) E. M. Holt, K. H. Whitmire, D. F. Shriver, *J. Am. Chem. Soc.* **1982**, *104*, 5621–5626; c) J. W. Kolis, E. M. Holt, D. F. Shriver, *J. Am. Chem. Soc.* **1983**, *105*, 7307–7313; d) C. P. Horowitz, D. F. Shriver, *J. Am. Chem. Soc.* **1985**, *107*, 8147–8153.
[38] E. Keller, SCHAKAL99, University of Freiburg, Germany, **1999**.
[39] G. M. Sheldrick, SADABS, Program for empirical absorption correction, University of Göttingen, Germany, **1996**.
[40] G. M. Sheldrick, SHELX97, Program for crystal structure determination, University of Göttingen, Germany, **1997**.

Received: September 25, 2007
Published online: December 13, 2007

